

- <sup>4</sup>V. Canuto and H. Chiu, *Phys. Rev.* **A2**, 518 (1970).  
<sup>5</sup>V. N. Sazonov and V. F. Tuganov, *Zh. Eksp. Teor. Fiz.* **67**, 2157 (1974) [*Sov. Phys. JETP* **40**, 1070 (1975)].  
<sup>6</sup>V. N. Sazonov and V. F. Tuganov, *Izv. Vyssh. Uchebn. Zaved., Radiofiz.*, **18**, 165 (1975).  
<sup>7</sup>J. Virtamo and P. Jauho, *Nuovo Cimento* **26B**, 537 (1975).  
<sup>8</sup>J. Virtamo and P. Jauho, *Astrophys. J.* **182**, 165 (1975).  
<sup>9</sup>A. V. Akopyan and V. N. Tsyтович, *Zh. Eksp. Teor. Fiz.* **71**, 166 (1976) [*Sov. Phys. JETP* **44**, 87 (1976)].  
<sup>10</sup>V. N. Tsyтович, *Tr. Fiz. Inst. Akad. Nauk SSSR* **66**, 191 (1973).  
<sup>11</sup>A. V. Akopyan and V. N. Tsyтович, *Fiz. Plazmy* **1**, 673 (1975) [*Sov. J. Plasma Physics* **1**, 371 (1975)].  
<sup>12</sup>Yu. M. Loskutov and V. V. Skobelev, *Vestn. Mosk. Gos. Univ., Ser. III, Fiz. Astr.* **16**, 721 (1975).  
<sup>13</sup>V. N. Tsyтович, *Teoriya turbulentnoy plazmy*, (Theory of Turbulent Plasmas), Atomizdat, 1971.  
<sup>14</sup>M. L. Ter-Mikaelyan, *Vliyaniye sredy na élektromagnetye protsessy privysokikh énergiyakh* (Effects of the Medium on High-Energy Electromagnetic Processes), *Izd. Akad. Nauk Arm. SSR*, Yerevan, 1969.  
<sup>15</sup>D. Melrose, *Astrophys. Space Sci.* **18**, 267 (1972).  
<sup>16</sup>V. L. Ginzburg and V. N. Tsyтович, *Zh. Eksp. Teor. Fiz.* **65**, 1818 (1973) [*Sov. Phys. JETP* **38**, 909 (1974)].  
<sup>17</sup>S. A. Kaplan and V. N. Tsyтович, *Plazmennaya astrofizika* (Plasma Astrophysics), Nauka, 1972.

Translated by W. H. Furry

## Study of the magnetic structure of the system $\text{Fe}_{65}(\text{Ni}_{1-x}\text{Mn}_x)_{35}$ by methods of magnetic scattering of neutrons and the Mössbauer effect

B. N. Mokhov, V. I. Goman'kov, V. A. Makarov, T. V. Sakharova, and N. I. Nugin

*Central Research Institute of Ferrous Metallurgy*  
 (Submitted April 20, 1976; resubmitted January 3, 1977)  
*Zh. Eksp. Teor. Fiz.* **72**, 1833-1844 (May 1977)

The magnetic structure of the system  $\text{Fe}_{65}(\text{Ni}_{1-x}\text{Mn}_x)_{35}$  with  $x = 0.14, 0.28$ , and  $0.37$  was investigated by the methods of magnetic scattering of neutrons in the temperature interval 4.2–700 K and the Mössbauer effect in an external field 45 kOe at 4.2 K. A joint analysis of the results shows that in the case of a concentration antiferro-ferromagnetic transition there is observed a broad spectrum of magnetic inhomogeneities, constituting the interacting regions in the antiferro-, ferro-, and paramagnetic states, and possibly also regions of "spin glass." The parameters of the ferromagnetic regions are determined and their polarization character is demonstrated, the Neel temperatures and the average magnetic moment per sublattice of the regions with antiferromagnetic order are estimated.

PACS numbers: 75.25.+z, 75.30.Kz, 76.80.+y

### INTRODUCTION

The study of the magnetic structure of the system  $\text{Fe}_{65}(\text{Ni}_{1-x}\text{Mn}_x)_{35}$  is of considerable interest from the point of view of the onset of the magnetically ordered state. As established by Shiga,<sup>[1]</sup> these alloys are ferromagnetic at  $x < 0.3$  and antiferromagnetic at  $x > 0.3$ . It is still unclear, however, how the magnetic order changes in this system, although this question has been the subject of a large number of studies. Thus, the presence of exchange anisotropy in the system and the temperature dependence of the magnetization have given grounds for the authors of<sup>[2,3]</sup> to suggest the coexistence of paramagnetic and antiferromagnetic regions at critical concentrations. At the same time, investigations of the magnetization in strong fields and at high pressures and investigations of the low-temperature specific heat and of the spontaneous magnetostrictions are treated in<sup>[4-7]</sup> under the assumption that the alloys are weak homogeneous collectivized ferromagnets. The Mössbauer spectra of the  $\text{Fe}^{57}$  nuclei,<sup>[8,9]</sup> to the contrary, show that the magnetic structure of the system is inhomogeneous to a considerable degree. Thus, direct

experimental investigations of the magnetic structure in the transition region of the concentrations are necessary.

In a preceding study,<sup>[10]</sup> magnetic scattering of neutrons was used to confirm the assumption that regions with ferromagnetic and antiferromagnetic types of order coexist in alloys with  $x = 0.28$  and  $0.37$ , and the polarization character of the ferromagnetic regions was demonstrated. The present paper is devoted to a further study of the singularities of the magnetic structure of the system  $\text{Fe}_{65}(\text{Ni}_{1-x}\text{Mn}_x)_{35}$  at critical concentrations, by the methods of magnetic scattering of neutrons and of the Mössbauer effect.

### 1. MEASUREMENT PROCEDURE AND SAMPLES

Neutron diffraction was investigated with a diffractometer with a wavelength  $\lambda = 1.07 \text{ \AA}$  in the angle interval  $10^\circ \leq 2\theta \leq 55^\circ$ . Small-angle scattering of the neutrons was investigated with a diffractometer with  $\lambda = 1.59 \text{ \AA}$ . The measurements were carried out on cylindrical polycrystalline samples of 8 mm diameter and

TABLE I.

Sample No.	Fe, at. %	Mn, at. %	Ni, at. %	$x$	$\mu_a, \mu_B$	$V_a/V, \%$	$T_N, K$
100	65.0	35.0	0	1.0	1.85±0.10	100	450
37	62.4	14.0	23.6	0.37	0.65±0.10	12	100
28	64.9	9.8	25.3	0.28	0.59±0.10	7	11
14	64.2	5.1	30.7	0.14	—	—	—

70 mm length in the temperature range from 4.2 to 700 K. All the samples were quenched in water after annealing at 1000 °C for 24 hours and had a single-phase fcc structure down to 4.2 K. The compositions of the investigated alloys are given in Table I.

The intensities of the small-angle scattering observed for samples 14, 28, and 37 had characteristic temperature dependences, which tended for the different compositions to a common value of the nuclear scattering at  $T > 700$  K. This is evidence of the magnetic origin of the small-angle scattering of the neutrons. The intensities of the small-angle magnetic scattering were obtained by subtracting from the experimental curves the temperature-independent scattering from a sample with  $x = 1.0$ . In the calculation of the cross sections of the magnetic small-angle scattering we used a standard vanadium sample. The collimation corrections turned out to be small, and the effects of inelastic scattering at small angles could be neglected at  $2\theta > 1^\circ$ .

The samples for the Mössbauer investigations were foils 25  $\mu\text{m}$  thick with natural  $\text{Fe}^{57}$  content and were obtained by rolling same ingots from which the samples were prepared for the neutron-diffraction measurements. The Mössbauer effect was investigated at 4.2 K in a transmission geometry using a spectrometer of an electrodynamic type with a scintillation detector, and AI-256 analyzer, and a  $\text{Co}^{57}(\text{Cr})$  source kept at room temperature. We used external magnetic fields of intensity 45 kOe, produced by a superconducting solenoid. The field was directed parallel to the flux of the quanta. In the measurements in the magnetic fields, the detector used was a proportional counter filled with Ar gas with methane additive.

## II. MAGNETIC SCATTERING OF NEUTRONS

1. *Antiferromagnetism.* Figure 1a shows parts of neutron diffraction patterns of alloys 37 and 28, measured at 4.2 K. The neutron diffraction patterns of alloys 100, 37, and 28 show, besides the principal nuclear reflections at  $2\theta = 24^\circ 30'$ , also superstructure magnetic reflections (110), which characterize the long-range antiferromagnetic order and which vanish with increasing temperature. For these alloys, in analogy with<sup>[11]</sup>, we propose a cubic noncollinear spin structure of the type  $\gamma\text{-FeMn}$ .<sup>[12]</sup> With decreasing  $x$ , the antiferromagnetic reflection broadens and decreases, and no antiferromagnetic reflections were observed on the neutron diffraction pattern of sample 14. The extent of the regions of antiferromagnetic coherent scattering, estimated from the half-width of the reflection (110) on Fig. 1a, is more than 350 and 100 Å for the alloys 37 and 28, respectively. The average sublattice moment

$\mu_a$  at 4.2 K was calculated, using the magnetic structure factor from<sup>[12]</sup>, from the ratio of the integral intensities of (110) and (220).

The values of  $\mu_a$  in Table I, in conjunction with the data of<sup>[11]</sup>, represent the concentration dependence of  $\mu_a$ , which offers evidence of the absence of an abrupt decrease of  $\mu_a$  at  $x < 0.5$ . Extrapolation of the concentration dependence of  $\mu_a$  into the region of ferromagnetic compositions with  $x < 0.28$  then yields nonzero values of  $\mu_a$  for sample 14 and the remaining alloys of this group, including the "classical" Invar composition  $\text{Fe}_{65}\text{Ni}_{35}$  ( $x = 0$ ). It can be assumed on the basis of this extrapolation that in the absence of long-range antiferromagnetic order<sup>[13]</sup> local antiferromagnetism is present in ferromagnetic alloys with  $x < 0.28$ . Just as in<sup>[13]</sup>, it is assumed that the local antiferromagnetism is confined to the first coordination sphere. The magnetic moment of the central Fe or Mn atom is then oriented opposite to the magnetic moments of the Fe and Mn atoms making up the first sphere.

According to the concentration dependence of  $\mu_a$ ,<sup>[11]</sup> the value of  $\mu_a$  remains constant in the interval  $0.6 < x \leq 1$  and decreases at  $x < 0.6$ . The latter may be due to the decrease of the volume fraction  $V_a/V$  of the regions of long-range antiferromagnetic order.<sup>[10]</sup> From the ratio of the integrated intensities of (110) and (220), at a constant value of  $\mu_a = 1.85\mu_B$ , we then calculate the values of  $V_a/V$  given in Table I.

Figures 1b and 1c show the temperature dependences of the peak intensity of the (110) reflections, from which the values of  $T_N$  listed in Table I are determined. The values of  $T_N$  of the alloys 100 and 37 agree well with the results of magnetic measurements, while  $T_N$  of alloy 28 correlates with the values of the temperatures at which the anomalous decrease of the magnetization is observed.<sup>[1]</sup> The intensities of the smeared-out maxima, which apparently are due to short-range antiferromagnetic order, are preserved above  $T_N$  in Figs. 1b and 1c.

Thus, a well-developed long-range antiferromagnetic

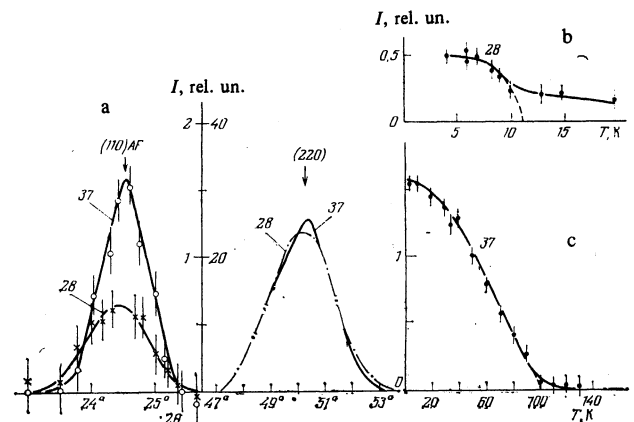


FIG. 1. Neutron diffraction patterns of antiferromagnetic alloys at 4.2 K (a) and temperature dependence of the peak intensity of the magnetic reflection (110) (b, c).

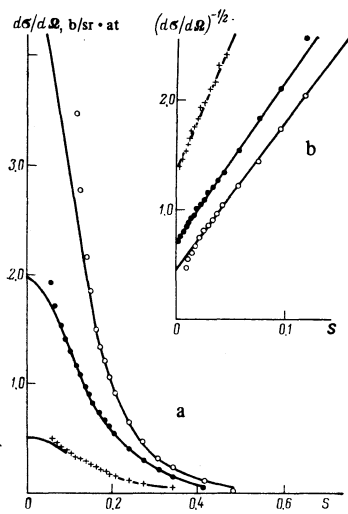


FIG. 2. Cross section of small-angle magnetic scattering of neutrons at 4.2 K; ○—alloy 14, ●—alloy 28, +—alloy 37.

$$M(s) = M(0) / (1 + \kappa^2 s^2), \quad (3)$$

where  $1/\kappa$  is the parameter of the dimension of the inhomogeneity,  $M(0)$  is the average magnetic moment over the region. This form of the  $M(s)$  dependence points to a polarization character of the variation of  $\rho'(r)$ . The values of  $(d\sigma/d\Omega)_0$  and  $\kappa$ , obtained from the data of Fig. 2b, are given in Table II. The calculated dependence of  $d\sigma/d\Omega$  on  $s$  is shown in Fig. 2a by solid lines.

To calculate  $C$  and  $M(0)$  the results were reduced by the method of<sup>[14]</sup>, with  $C = n/N$ , where  $n$  is the number of ferromagnetic regions and  $N$  is the total number of atoms of the sample. In the absence of overlap of the regions, the average magnetic moment of the atom  $\bar{\mu}$  is then

$$\bar{\mu} = CM(0) \quad (4)$$

order is observed in the alloys 100, 37, and 28. The value of  $T_N$  of the alloy 28 (Table I) does not agree with the conclusion of<sup>[3]</sup> that there is no  $T_N < 100$  K in the transition region of concentrations.

**2. Ferromagnetic regions.** The angular dependence of the cross sections of the small-angle magnetic scattering of neutrons by samples 14, 28, and 37 is shown in Fig. 2a, where  $s = 4\pi \sin\theta/\lambda$ . The small-angle scattering is observed in alloys 37 and 28 below  $T_N$  and is maximal in the ferromagnetic sample 14. Thus, magnetic inhomogeneities exist in the antiferromagnetic alloys 37 and 28 and in the ferromagnetic alloy 14. When choosing the magnetic model of the alloys, account is taken of the values of the average magnetic moment  $\bar{\mu}$  and of the Curie temperature  $T_c$  of the alloy. The values of  $\bar{\mu}$  obtained by interpolating the data of<sup>[2]</sup>, and the values of  $T_c$  measured in our investigations are given in Table II.

According to<sup>[2]</sup>, the value of  $\bar{\mu}$  of sample 37 is at the measurement-error level, although there is no  $T_c$  and  $T_N = 100$  K (Table I). The values of  $\bar{\mu}$  and  $T_c$  of alloy 28 are given in Table II. It is known also that exchange anisotropy is observed in these alloys.<sup>[2]</sup> It can therefore be assumed that the observed small-angle scattering in the alloys 37 and 28 is due to scattering by ferromagnetic regions, since the antiferromagnetic—ferromagnetic transition is not accompanied by a change in the forward scattering.<sup>[18]</sup> Thus, the inhomogeneities in alloys 37 and 28 are ferromagnetic regions and the cross section takes accordingly the form<sup>[14]</sup>

$$d\sigma/d\Omega = 0.0486C(1-C)[M(s)]^2, \quad (1)$$

where  $C$  is the concentration of the ferromagnetic regions while

$$M(s) = \int_V \rho'(r) \exp(i\mathbf{r} \cdot \mathbf{s}) dr, \quad (2)$$

and  $\rho'(r)$  is the density of the magnetic moment in the region. The linear dependence of  $(d\sigma/d\Omega)^{-1/2}$  on  $s^2$ , shown in Fig. 2b, enables us to describe  $M(s)$  by a Lorentzian<sup>[14]</sup>

and the simultaneous solution of Eq. (1) at  $s=0$  and Eq. (4) yields the values  $C = (0.08 \pm 0.01)\%$  and  $M(0) = 230 \pm 20 \mu_B$  for the alloy 28. The value of  $C$  for alloy 28 is of the same order as the probability of formation of clusters that are due to the fluctuations of the concentration in the alloy and contain from 9 to 12 nickel atoms in the first coordination sphere of the atoms Fe and Mn. It appears that these clusters produce ferromagnetic-polarization regions that are the seeds of ferromagnetism in the alloys.

In the spherical approximation, using (2) and (3), the density of the magnetic moment in the region of the ferromagnetic polarization takes the form

$$\rho'(r) = \frac{M(0)\kappa^3}{4\pi r} e^{-\kappa r}. \quad (5)$$

Figure 3 shows the radial distribution of the density of the magnetic moment for the alloy 28 at 4.2 K, calculated for ten coordination spheres. The moment decreases by one order of magnitude from the first to the tenth coordination sphere. The minimal radius of inertia of the region, calculated from Fig. 2a in the Guinier approximation<sup>[16]</sup> is  $7.3 \text{ \AA}$ , and corresponds to the dimensions of propagation of the magnetic polarization of Fig. 3.

Since there is no long-range antiferromagnetic order in sample 14 and  $T_c = 265$  K, the matrix of the alloy is ferromagnetic. The magnetic inhomogeneities that lead to small-angle scattering have here a different character than the inhomogeneities of the alloys 37 and 28. Equation (1) describes in this case the scattering by in-

TABLE II.

Sample No.	$T$ , K	$(d\sigma/d\Omega)_0$ , b/sr·at	$\kappa$ , $\text{\AA}^{-1}$	$\bar{\mu}$ , $\mu_B$	$T_c$ , K
37	4.2	$0.52 \pm 0.05$	$0.24 \pm 0.01$	0.01	—
	77.0	$0.41 \pm 0.04$	$0.24 \pm 0.01$	—	—
	295.0	$0.30 \pm 0.03$	$0.27 \pm 0.01$	—	—
28	4.2	$1.98 \pm 0.20$	$0.22 \pm 0.01$	0.18	70
	77.0	$1.79 \pm 0.20$	$0.23 \pm 0.01$	—	—
	295.0	$0.29 \pm 0.03$	$0.30 \pm 0.01$	—	—
14	4.2	$4.94 \pm 0.50$	$0.18 \pm 0.01$	0.96	265
	77.0	$2.32 \pm 0.20$	$0.21 \pm 0.01$	—	—
	295.0	$3.85 \pm 0.40$	$0.18 \pm 0.01$	—	—

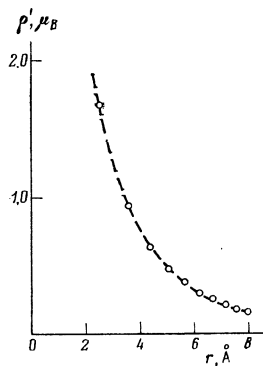


FIG. 3. Radial distribution of the density of the magnetic moment of the alloy 28 at 4.2 K.

homogeneities as a result of the negative perturbation of the magnetic moments of the ferromagnetic matrix.<sup>[15]</sup> In this case  $C$  denotes the concentration of regions with decreased moment. Then, in analogy with<sup>[13]</sup>, it can be assumed that the negative perturbations are produced around clusters consisting only of Fe and Mn atoms situated in the first coordination sphere around the Fe and Mn atoms. Their concentrations, calculated in accordance with the binomial distribution for the given composition is  $C=1.2\%$ , and the average total decrease of the moment of the perturbed region is  $M(0)=50\mu_B$ . It appears that the local antiferromagnetism assumed above is realized in these clusters.

Thus, the change of the magnetic order in the investigated system proceeds via formation of separate ferromagnetic regions in the antiferromagnetic alloys 37 and 28, while the overlap of these regions produces in alloy 14 a long-range ferromagnetic order where, however, the existence of local antiferromagnetism is possible.

3. *Temperature dependences of small-angle scattering.* Additional information on the character and interactions of the magnetic inhomogeneities in the system is obtained from the temperature dependences of the small-angle scattering of the neutrons, as shown in Fig. 4.

For sample 14 we see the characteristic peak of the critical scattering, corresponding to  $T_c$  of this composition. The curves on Fig. 4 have the following singularities: 1) the cross sections are insensitive to the antiferromagnetic transformation in alloys 37 and 28 at  $T_N$  and there are no characteristic maxima of the critical scattering; 2) the cross sections of the alloy 28 are constant in the temperature interval  $4.2 \leq T \leq 50$  K; 3) the cross sections in sample 14 decrease "anomalously" when the temperature is raised to 70 K.

The values of  $(d\sigma/d\Omega)_0$  and  $\kappa$  for some temperatures are given in Table II.

The decrease of  $d\sigma/d\Omega$  of samples 37 and 28 with decreasing temperature in Fig. 4 is similar to the behavior of the temperature dependence, observed in<sup>[17]</sup>, of the critical scattering. The absence of a maximum of the critical scattering of samples 37 and 28 shows that the ferromagnetic regions of the polarization do not produce a long-range ferromagnetic order, so that when the temperature is increased individual regions with

local Curie temperatures go over into the paramagnetic state. Within the limits of the experimental errors, the curve for the alloy 37 on Fig. 4 cannot be used to determine the value of the local  $T_c$ . However, an abrupt decrease of  $d\sigma/d\Omega$  is observed on the temperature dependence of  $d\sigma/d\Omega$  of sample 28 above 70 K, and this enables us to estimate the local Curie temperature at  $\approx 70$  K.

The "anomalous" decrease of the cross sections of alloy 14 in the interval 4.2–70 K on Fig. 4 point to a decrease in the fraction of regions with decreased values of the magnetic moments. This can be due to a transition of the regions with local antiferromagnetism into the paramagnetic state, with simultaneous polarization of these regions by the surrounding ferromagnetic matrix. Thus, the local antiferromagnetism causes partial depolarization of the ferromagnetic matrix at 4.2 K; this depolarization vanishes when the temperature is raised to 70 K. The increase of the ferromagnetic polarization is evidenced also by the increase of  $\kappa$  (Table II) in this temperature interval. The usual growth of  $d\sigma/d\Omega$  and the decrease of  $\kappa$  (Table II) in the ferromagnetic matrix as  $T_c$  is approached are observed in Fig. 4 when the temperature is increased from 100 to 265 K.

### III. THE MÖSSBAUER EFFECT

The spectra of the investigated alloys at 4.2 K are shown in Fig. 5. The spectrum of the ferromagnetic alloy 14 (Fig. 5a) corresponds to a large set of components, each of which constitute a system of lines of magnetic hyperfine splitting and is characterized by a magnetic field intensity  $H_{\text{eff}}$ . The values of the maximum  $H_{\text{eff}}$  estimated from the positions of the resolved outer-

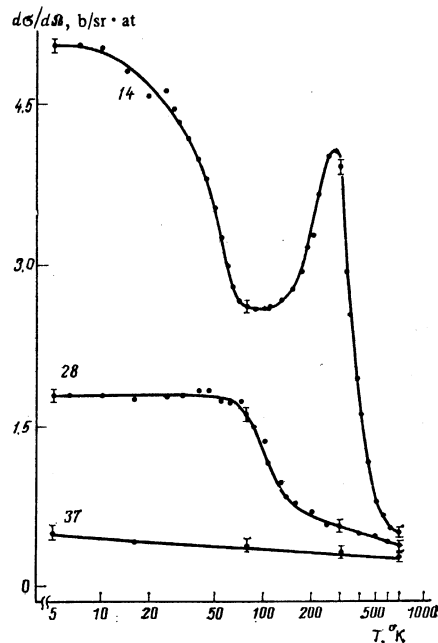


FIG. 4. Temperature dependence of small-angle magnetic scattering at a fixed angle.  $2\theta=1^\circ30'$ ,  $1^\circ15'$  and  $1^\circ15'$  for samples 14, 28, and 37, respectively.

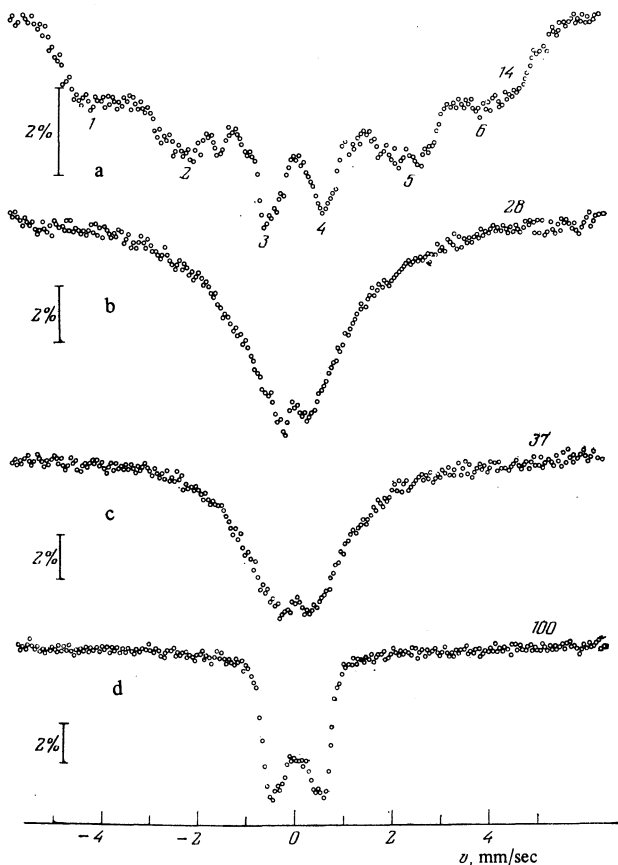


FIG. 5. Mössbauer spectra of the alloys 14 (a), 28 (b), 37 (c), and 100 (d) at 4.2 K in the absence of an external magnetic field.

most lines are quite large and amount to 250 kOe. From the form of the spectrum it can be also assumed that the values of the minimal  $H_{\text{eff}}$  are close to zero. Thus, the distribution of  $H_{\text{eff}}$  in this sample is unusually broad.

The spectrum of the antiferromagnetic alloy 100 (Fig. 5d) is much narrower than the spectrum of the alloy 14, and the value of  $H_{\text{eff}}$  in this spectrum does not exceed 40 kOe. Similar values of  $H_{\text{eff}}$  were observed in the spectra of binary antiferromagnetic Fe-Mn alloys.<sup>[19]</sup> The spectral lines of alloys 28 and 37 (Figs. 5b and 5c) are much more poorly resolved, so that it is impossible to present a simple interpretation.

To investigate in greater detail the distribution of  $H_{\text{eff}}$ , the spectra of the alloys 28 and 14 were measured in a magnetic field of intensity 45 kOe. They are shown in Figs. 6a and 6c, respectively. Comparison of Figs. 5 and 6 shows that the external magnetic field alters significantly the form of the spectrum. It can be noted that in the spectra of the alloy 14 in an external field, the distance between lines 1 and 6 decreases, while the lines 2 and 5 are strongly suppressed. In the spectrum of the alloy 28, the wings become narrower, but broadening of the central part takes place. The appreciable decrease of the intensities of the lines 2 and 5 in the spectra of the alloy 14 indicates that the atomic magnetic moments of Fe are oriented parallel to the external field.

To obtain quantitative data, the spectra shown in Fig. 6 were reduced with an ES-1020 computer by the method proposed by Hesse and Rubartsch in<sup>[20]</sup>. The calculations were carried out for the left halves of the spectra. The spectra were resolved into 65 components under the assumption that all the lines have a Lorentz shape 0.35 mm/sec wide, the isomeric shifts are the same for all components, and there is no quadrupole splitting. These assumptions are apparently valid, since the spectra in Fig. 6 are practically symmetrical. The ratio of the spectral line intensities is determined by the orientation of the atomic magnetic moment relative to the external field. This ratio was assumed to be 3:0:1:1:0:3 for all components, as is required for a ferromagnetic sample that is fully polarized by an external field. This ratio is subject to no doubt for the spectrum of the alloy 14. It is, however, not the only one possible in the case of the alloy 28, since it contains besides the ferromagnetic regions also regions with long-range antiferromagnetic order. The orientation of the atomic magnetic moment in these regions depends on many factors, principal among which are the crystal and exchange anisotropy and the external field itself. The exchange anisotropy contributes to the collinear arrangement of the moments in the ferromagnetic and antiferromagnetic regions, and the external magnetic field increases the angle between them. It is impossible to take correct account of the action of both factors, or to estimate the role of the crystal anisotropy for such a complicated system as the alloy 28. Thus, the direction of the magnetic moments in antiferromagnetic regions remains indeterminate. It is seen from Table I, however, that the exchange fraction of the antiferromagnetic regions in the alloy 28 is small. It appears that the contributions of these regions themselves to the Mössbauer spectrum can be neglected. We also assume that by virtue of the smallness the volume fraction and the large value of the external magnetic field we can ignore the disorienting influence of the antiferromagnetic regions on the ferromagnetic ones.

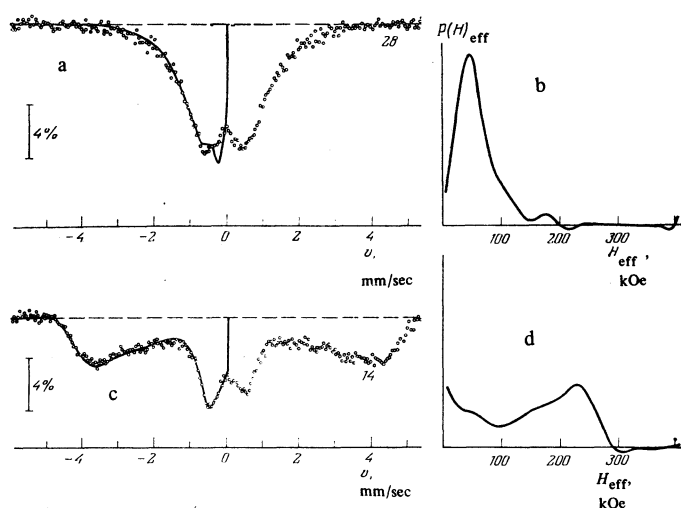


FIG. 6. Mössbauer spectra of the alloys 28 (a) and 14 (c) at 4.2 K in an external magnetic field of 45 kOe, and the corresponding distributions of the effective fields (b, d).

The results of the reduction of the spectra are shown in Figs. 6b and 6d. The function  $P(H_{\text{eff}})$  represents the relative intensity of the components and is the probability density for the distribution  $H_{\text{eff}}$ . The solid lines in Figs. 6a and 6c represent the left halves of the spectra, calculated from the functions  $P(H_{\text{eff}})$ . They agree satisfactorily with the experimental spectra. The horizontal line on Figs. 6a and 6c shows the selected background level.

The function  $P(H_{\text{eff}})$  for the alloy 28 is shown in Fig. 6b. It consists of two unresolved maxima. The top of the first maximum occurs at  $H_{\text{eff}}$ , which coincides with the external field. The position of the top together with the broadening of the central part of the spectrum in the magnetic field allow us to conclude that the greater part of the Fe atoms is in the paramagnetic state. Indeed, the broadening of the spectrum indicates an increase of  $H_{\text{eff}}$  for the corresponding Fe atoms, while the fact that  $H_{\text{eff}}$  of the top of the first maximum coincides with the value of the external field indicates the contribution made to  $H_{\text{eff}}$  by the atomic magnetic moment is negligibly small. This situation is typical of spectra of paramagnets in external magnetic fields. It appears that in the alloy 28 at 4.2 K there exist paramagnetic regions in which an appreciable fraction of the Fe atoms is located.

At the same time, the first maximum of  $P(H_{\text{eff}})$  cannot be attributed only to the presence of paramagnetic Fe atoms. Its width is at least double the value obtained in the original paper of Hesse and Rubartsch<sup>[20]</sup> for the purely paramagnetic state. Although it is difficult to explain unambiguously the causes of the broadening, we propose that it is caused by the Fe atoms, for which there exists an additional contribution to  $H_{\text{eff}}$  from their magnetization. By atomic magnetization is meant the time-average value of the projection of the magnetic moment on the local quantization axis. If we assume further that the magnetizations of the individual atoms are relatively small and their directions are randomly distributed relative to direction of the external field, then we obtain as a result a broadening of the peak of  $P(H_{\text{eff}})$  of the paramagnetic atoms, but the peak retains its symmetrical shape. It is interesting to note that similar properties are possessed by "spin glass," which is produced as an intermediate state between paramagnetism and ferromagnetism. Above the "freezing" temperature, "spin glass" is a paramagnet, and lowering the temperature leads to "freezing" of the atomic magnetic moments along the direction of the local anisotropy. There is no long-range magnetic order in such a system.

Another possible cause of the broadening of the peak  $P(H_{\text{eff}})$  may be due to relaxation of the atomic moment in the magnetic field. This explanation, however, seems less probable, for in this case an intense paramagnetic line should be observed in the spectra obtained without the magnetic field, and this is not seen in Fig. 6a.

The second maximum of  $P(H_{\text{eff}})$  in Fig. 6b is located in the region  $H_{\text{eff}} = 100$  kOe and corresponds to the Fe atoms, for which  $H_{\text{eff}}$  decreases when the external mag-

netic field is turned on. This follows from the narrowing of the wings of the spectrum in the magnetic field. The magnetic moments of these Fe atoms are ferromagnetically ordered. Thus, in alloy 28 the greater part of the Fe atoms is contained in the paramagnetic regions, and possibly in the "spin-glass" regions. The remaining Fe atoms are in the regions with ferromagnetic order.

The function  $P(H_{\text{eff}})$  for the alloy 14 (Fig. 6d) consists of two broad well resolved maxima. A similar form of  $P(H_{\text{eff}})$  was obtained by Shiga, Maeda, and Nakamura<sup>[9]</sup> for an alloy having a close composition in a magnetic field 50 kOe. They attribute the maximum in the region of the zero values of  $H_{\text{eff}}$  to the antiferromagnetic regions.<sup>[9]</sup> According to neutron-diffraction data, however, there is no long-range antiferromagnetic order in alloy 14. We therefore propose that the function  $P(H_{\text{eff}})$  for this alloy reflect the distribution of the atomic magnetization of Fe. The maximum of  $P(H_{\text{eff}})$  near the zero values of  $H_{\text{eff}}$  corresponds to Fe atoms characterized by small magnetization.

The second maximum of  $P(H_{\text{eff}})$  at  $H_{\text{eff}} = 220$  kOe in Fig. 6d definitely corresponds to Fe atoms in the ferromagnetic state. Indeed, application of an external field decreases the values of the maximum fields from 250 to 220 kOe, which approximately coincides with the value of the external field, decreased by the demagnetizing field of the sample. The large width of the second maximum of  $P(H_{\text{eff}})$  is probably due to the dependence of the value of the atomic moment of Fe on the composition of the nearest environment.

#### IV. CONCLUSIONS

A joint analysis of the results on the magnetic scattering of the neutrons and on the Mössbauer effect makes it possible to present a model of the magnetic structure of the system undergoing a concentration transition from the antiferromagnetic into the ferromagnetic state. According to the neutron diffraction data, the alloys 37 and 28 contain regions with long-range antiferromagnetic order as well as ferromagnetic regions. The latter are made up of clusters that polarize the matrix. The data on the Mössbauer effect of the alloy 28 confirm the existence of ferromagnetic regions, and also point to the presence in this alloy of paramagnetic regions, and possible of "spin glass" regions. We note that the experimentally established magnetic structure of alloys 37 and 28 agrees with the theoretical premises,<sup>[21]</sup> according to which systems that are characterized by a random distribution of the exchange integral of the nearest neighbors can have a magnetic phase diagram on which the concentration region of the ferromagnetic state is separated from the paramagnetic region by a "spin glass" region.

On going from alloy 37 to alloy 28, the number of ferromagnetic regions increases, causing them to overlap in the alloy 14 and causing establishment of long-range ferromagnetic order with clearly pronounced  $T_c$ . No regions with long-range antiferromagnetic order were observed in alloy 14. However, the form of the

function  $P(H_{eff})$  at 4.2 K indicates that the magnetization of alloy 14 is spatially inhomogeneous. On the other hand, the anomalies of the temperature dependence of  $d\sigma/d\Omega$  allows us to conclude that this inhomogeneity is due to the depolarizing influence of the local antiferromagnetism.

- <sup>1</sup>M. Shiga, J. Phys. Soc. Jpn. 22, 539 (1967).  
<sup>2</sup>Y. Nakamura and N. Miyata, J. Phys. Soc. Jpn. 23, 223 (1967).  
<sup>3</sup>A. Z. Men'shikov, V. A. Kazantsev, and N. N. Kuz'min, Pis'ma Zh. Eksp. Teor. Fiz. 23, 6 (1976) [JETP Lett. 23, 4 (1976)].  
<sup>4</sup>B. K. Ponomarev and S. V. Aleksandrovich, Zh. Eksp. Teor. Fiz. 67, 1965 (1974) [Sov. Phys. JETP 40, 976 (1975)].  
<sup>5</sup>Y. Nakamura, M. Hayase, M. Shiga, Y. Miyamoto, and N. Kawai, J. Phys. Soc. Jpn. 30, 720 (1971).  
<sup>6</sup>S. Kawarazaki, M. Shiga, and Y. Nakamura, Phys. Status Solidi B 50, 359 (1972).  
<sup>7</sup>M. Hayase, M. Shiga, and Y. Nakamura, J. Phys. Soc. Jpn. 30, 729 (1971).  
<sup>8</sup>I. N. Nikolaev, V. A. Makarov, I. M. Puzel', and L. S. Pavlyukov, Fiz. Metal. Metalloved. 35, 1305 (1973).  
<sup>9</sup>M. Shiga, I. Maeda, and Y. Nakamura, J. Phys. Soc. Jpn. 37, 363 (1974).

- <sup>10</sup>V. I. Goman'kov, B. N. Mokhov, and E. I. Mal'tsev, Pis'ma Zh. Eksp. Teor. Fiz. 23, 97 (1976) [JETP Lett. 23, 83 (1976)].  
<sup>11</sup>Y. Nakamura, M. Shiga, and Y. Takeda, J. Phys. Soc. Jpn. 27, 1470 (1969).  
<sup>12</sup>H. Umebayashi and Y. Ishikawa, J. Phys. Soc. Jpn. 26, 1289 (1966).  
<sup>13</sup>V. I. Goman'kov, E. V. Kozis, and B. N. Mokhov, Dokl. Akad. Nauk SSSR 225, 807 (1975) [Sov. Phys. Dokl. 20, 843 (1975)].  
<sup>14</sup>T. J. Hicks, B. Rainford, J. S. Kouvel, G. G. Low, and J. B. Comly, Phys. Rev. Lett. 22, 531 (1969).  
<sup>15</sup>J. B. Comly, T. M. Holden, and G. G. Low, J. Phys. C 1, 485 (1968).  
<sup>16</sup>A. Guinier, X-Ray Diffraction of Crystals, Freeman, 1963.  
<sup>17</sup>E. Z. Valiev, A. V. Doroshenko, S. K. Sidorov, Yu. M. Nikulin, and S. G. Teploukhov, Fiz. Metal. Metalloved. 38, 993 (1974).  
<sup>18</sup>Rasseyanie teplovykh neitronov (Scattering of Thermal Neutrons) Atomizdat, M., 1970.  
<sup>19</sup>Y. Ishikawa and Y. Endoh, J. Phys. Soc. Jpn. 23, 205 (1967).  
<sup>20</sup>J. Hesse and A. Robartsch, J. Phys. E 7, 526 (1974).  
<sup>21</sup>D. Sherrington and S. Kirkpatrick, Phys. Rev. Lett. 35, 1972 (1975).

Translated by J. G. Adashko

## Singularities of the thermodynamics of unsymmetrical disordered systems

Yu. Ya. Gurevich and Yu. I. Kharkats

*Institute of Electrochemistry, USSR Academy of Sciences*

(Submitted April 29, 1976)

Zh. Eksp. Teor. Fiz. 72, 1845-1857 (May 1977).

A theory is developed of phase transitions in asymmetrical disordered systems. A superionic crystal is considered by way of an example of such a system. Within the framework of the molecular-field approximation, expressions are obtained for the free energy and the equation of state. The state of the system depends on two dimensionless parameters, which are determined by the properties of the crystal. The specifics of the unsymmetrical system manifest itself in the fact that both single phase transitions and bitransitions are possible. New critical conditions corresponding to realization of bitransitions are obtained and expressions are derived for the corresponding temperatures.

PACS numbers: 64.60.Cn

This paper is devoted to a theoretical investigation of first-order phase transitions that can be realized in asymmetrical systems with disorder. The study of the singularities of the thermodynamics of model disordered systems, both symmetrical (for example, spin systems, AB alloys, certain lattice models of adsorption) and asymmetrical (for example,  $A_nB_m$  alloys, superionic crystals) has been the subject of many papers.<sup>[1-6]</sup> At the same time, some asymmetrical systems should have a number of interesting singularities, which have not been considered earlier. In particular, as will be shown below, two genetically related phase transitions—bitransitions—may take place in such systems.

### 1. FORMULATION OF PROBLEM

An example of an asymmetrical system to be considered is a superionic crystal, although, as will be shown subsequently, the results are general in character and can be used also for the description of a rather large class of objects and phenomena.

Superionic crystals, which have been intensively investigated of late, are a special class of ionic crystals. One of the most characteristic features of these crystals is the jumplike changes of the ionic conductivity, by several times or by several orders of magnitude.